



ELSEVIER

Contents lists available at ScienceDirect

Electrochimica Acta

journal homepage: [www.elsevier.com/locate/electacta](http://www.elsevier.com/locate/electacta)

# A high performance redox-mediated electrolyte for improving properties of metal oxides based pseudocapacitive materials



Wei Han<sup>a</sup>, Ling-Bin Kong<sup>a,b,\*</sup>, Mao-Cheng Liu<sup>b</sup>, Dan Wang<sup>b</sup>, Jia-Jia Li<sup>b</sup>, Long Kang<sup>b</sup>

<sup>a</sup> State Key Laboratory of Advanced Processing and Recycling of Non-ferrous Metals, Lanzhou University of Technology, Lanzhou 730050, PR China<sup>1</sup>

<sup>b</sup> School of Materials Science and Engineering, Lanzhou University of Technology, Lanzhou 730050, PR China<sup>1</sup>

## ARTICLE INFO

### Article history:

Received 19 September 2015

Received in revised form 23 October 2015

Accepted 26 October 2015

Available online 30 October 2015

### Keywords:

Redox electrolyte

Sodium persulfate

Supercapacitor

## ABSTRACT

A novel redox-mediated aqueous electrolyte is prepared by adding sodium persulfate ( $\text{Na}_2\text{S}_2\text{O}_8$ ) into KOH alkaline electrolyte for the application in most metal oxide based supercapacitors. The electrochemical behaviors of nickel oxide (NiO) electrode in 2 M KOH and 2 M KOH containing different concentration of  $\text{Na}_2\text{S}_2\text{O}_8$  electrolytes, respectively, were characterized by cyclic voltammetry and electrochemical impedance spectroscopy methods. The results indicate that the reaction mechanism of NiO electrode in  $\text{Na}_2\text{S}_2\text{O}_8$  mixed electrolytes appears to be the reversible redox of  $\text{Ni}^{2+}$  to  $\text{Ni}^{3+}$  on two different channels, which is different with that in KOH electrolyte. Charge-discharge experiments show that the discharge ability of the NiO electrode in redox electrolyte is excellent. When added  $\text{Na}_2\text{S}_2\text{O}_8$  into KOH electrolyte, the charge time is shorted and the discharge time is increased sharply. The specific capacitance was up to  $6317.5 \text{ F g}^{-1}$  at  $0.5 \text{ A g}^{-1}$  in mixed 2 M KOH and 0.03 M  $\text{Na}_2\text{S}_2\text{O}_8$ , more than 100% coulombic efficiency. Fortunately, this new redox-mediated aqueous electrolyte not only suitable for the metal oxide based electrode, but also have much effect to the metal sulfide, vanadate, and phosphate electrode et al.

© 2015 Elsevier Ltd. All rights reserved.

## 1. Introduction

In the search for novel energy storage solutions, electrochemical capacitors (ECs) have become prominent as an important and rapidly growing class of devices, which are expected to exhibit the desirable properties of high power density, fast charging, and long cycling life. Such outstanding properties make them promising energy storage devices, such as in hybrid electric vehicles, mobile electronic devices, large industrial equipment, memory backup systems, and military devices [1–4]. However, the disadvantage of ECs including low energy densities and high cost has been identified as a major challenge for the capacitive storage science [5].

To overcome these limitations, significant efforts have been focused on the enhancement of the energy density to make it comparable to that of batteries [6,7]. An effective method is to develop transition metal oxides or conducting polymer based Faradic pseudocapacitors to replace the electric double-layer capacitors based on carbons [8]. Conducting polymers have shown high pseudocapacitance but poor stability during the charge-discharge cycling [9–11]. Therefore, transition metal oxides are

considered to be one of the most promising materials for ECs [12–15]. Metal oxides possess multiple oxidation states that enable rich redox reactions for pseudocapacitance, and it has drawn extensive attention in pseudocapacitors [16]. Hence, there are numerous reports have been explored using transition metal oxides, hydroxides and nitrides that includes  $\text{RuO}_2$  [17],  $\text{CuO}$  [18],  $\text{TiO}_2$  [19],  $\text{Co}_3\text{O}_4$  [20],  $\text{MnO}_2$  [21],  $\text{SnO}_2$  [22],  $\alpha\text{-MnMoO}_4$  [23],  $\text{NiCo}_2\text{O}_4$  [24],  $\text{Co}_3\text{S}_4$  [25],  $\text{V}_2\text{O}_5$  [26],  $\text{VN}$  [27],  $\text{Ni(OH)}_2$  [28],  $\text{CoMoO}_4$  [29],  $\alpha\text{-Co(OH)}_2$  [30],  $\text{MoS}_2$  [31], etc, as the active electrodes for pseudocapacitors. Lang et al. [32] used a facile approach prepared loose-packed NiO nano-flakes material shows high power density at high rates of discharge and excellent cycle life, suggesting their potential application in supercapacitors.

It is well known that the electrode materials and the using of electrolyte are particularly critical in determining the performance of supercapacitors, the selection of electrode materials is very important, and the electrolyte is another important factor affecting the capacitance of a supercapacitor. An alternative method to enhance the capacitance of carbon material based supercapacitors has been reported through using a redox active electrolyte. Recently, there have been a few reports that redox additives were introduced into the electrolyte for carbon EDLCs to substantially enhance the capacitance via redox reactions of the additives between the electrode and electrolyte. For example, Roldan et al. [33] reported an increase in specific capacitance from 320 to

\* Corresponding author. Tel.: +86 931 2976579; fax: +86 931 2976578.

E-mail address: [konglb@lut.cn](mailto:konglb@lut.cn) (L.-B. Kong).

<sup>1</sup> <http://yuanxi.lut.cn/xny/>.

901  $\text{F g}^{-1}$  by adding hydroquinone to  $\text{H}_2\text{SO}_4$  electrolytes. Wu et al. [34] introduced phenylenediamine as a redox mediator into KOH electrolyte for the carbon-based supercapacitor, and a much higher specific capacitance (605.2  $\text{F g}^{-1}$  than that 144.0  $\text{F g}^{-1}$  in conventional KOH electrolyte) has been achieved. Senthilkumar et al. [35] used polyvinyl-alcohol  $\text{H}_2\text{SO}_4$  gel electrolyte with the addition of hydroquinone, the specific capacitance increased from 425 to 941  $\text{F g}^{-1}$ , they also reported potassium iodide addition into aqueous  $\text{H}_2\text{SO}_4$  electrolyte [36], the specific capacitance increased from 472 to 912  $\text{F g}^{-1}$ . The author believes these increases in capacitances were attributed to the rapid faradaic reactions at the electrode/electrolyte interface that occurred by introducing mediators (hydroquinone/quinine, iodide/iodine pairs) into electrolytes. The active electrolyte greatly improved the electric double-layer capacitance, fortunately, the active additives are also valid for pseudocapacitors, and there have been few reports on this investigation. Su et al. [37] reported an increase in specific capacitance of Co-Al layered double hydroxide electrode up to 712 and 317  $\text{F g}^{-1}$  at a current density of 2  $\text{A g}^{-1}$  by adding either  $\text{K}_3\text{Fe}(\text{CN})_6$  or  $\text{K}_4\text{Fe}(\text{CN})_6$  into KOH solution, which is higher than that of pure KOH solution (226  $\text{F g}^{-1}$ ). Zhao et al. [38] added  $\text{K}_3\text{Fe}(\text{CN})_6$  into KOH solution to increase the specific capacitance of Co(OH)<sub>2</sub>/graphene electrode, the specific capacitance can up to 7514  $\text{F g}^{-1}$  at 16  $\text{A g}^{-1}$ . As mentioned above, more attention has been paid to investigating either electrode or electrolyte to enhance the specific capacitance, but there is few efforts have been done to find a high performance redox-mediated electrolyte to improve the properties of metal oxides based pseudocapacitive materials.

Persulfates (specifically  $\text{Na}_2\text{S}_2\text{O}_8$ ) are strong oxidants that have been widely used in many industries for situ chemical oxidation of chlorinated and non-chlorinated organic, initiating emulsion polymerization reactions, clarifying swimming pools, hair bleaching, micro-etching of copper printed circuit boards, and TOC analysis [39–42]. In the last few years there has been increasing interest in sodium persulfate as an oxidant for the destruction of a broad range of soil and groundwater contaminants [43]. In addition to direct oxidation, sodium persulfate can be induced to form sulfate radicals, thereby providing free radical reaction mechanisms similar to the hydroxylradical pathways generated by Fenton's chemistry. These reactions are given by the equation (S1); the initiator can be the transition metal ions ( $\text{Fe}^{2+}$ ,  $\text{Ni}^{2+}$ ) and ultraviolet rays.

In this work,  $\text{Na}_2\text{S}_2\text{O}_8$  was used as a redox-mediated of alkaline electrolyte to improve the electrochemical property of transition

metal oxides electrode. The transition metal oxides electrode- $\text{Na}_2\text{S}_2\text{O}_8/\text{KOH}$  system shows an unusually high specific capacitance (the specific capacitance of NiO electrode was up to 6317.5  $\text{F g}^{-1}$  at 0.5  $\text{A g}^{-1}$  in mixed solution of 2 M KOH and 0.03 M  $\text{Na}_2\text{S}_2\text{O}_8$ ), and more than 100% coulombic efficiency. The electrochemical measurement testified that this new system is suitable for most metal oxides, sulfide and phosphate electrode et al., and they exhibit the same trait as the NiO electrode in  $\text{Na}_2\text{S}_2\text{O}_8/\text{KOH}$  electrolyte system. In addition to the specific capacitance was greatly promoted, it was also emerged a phenomenon of charging time shortened and the discharge time extended. This new electrochemical system is promising for further developments of metal oxides electrode (metal sulfide, vanadate, and phosphate electrode et al) of high performance supercapacitors.

## 2. Experimental Section

### 2.1. Electrolytes

Two types of electrolytes were used in the electrochemical evaluation, i.e., (1) 2 M KOH aqueous electrolyte; (2) a mixed solution containing 2 M KOH aqueous electrolyte and different concentrations (0.01, 0.02, 0.03, 0.04, and 0.05 M) of  $\text{Na}_2\text{S}_2\text{O}_8$ . In this work,  $\text{Na}_2\text{S}_2\text{O}_8$  was added into the conventional KOH electrolytes to increase the overall capacitance of electrode materials by taking advantage of the redox reactions of  $\text{Na}_2\text{S}_2\text{O}_8$ , when it comes to the inducing agents. The  $\text{Na}_2\text{S}_2\text{O}_8/\text{KOH}$  electrolytes were freshly prepared by dissolving the corresponding amounts of  $\text{Na}_2\text{S}_2\text{O}_8$  in 2 M KOH solution.

### 2.2. Electrode preparation and electrochemical characterization

Each electrode was composed as follows: 80 wt% of the active material was mixed with 7.5 wt% of acetylene black and 7.5 wt% of conducting graphite in an agate mortar until a homogeneous black powder was obtained. 5 wt% of poly (tetrafluoroethylene) was added together with a few drops of ethanol. The resulting paste was pressed at 10 MPa into an open-cell nickel foam (ChangSha Lyrun New Material Co. Ltd, grade 90 PPI (pores per linear inch), 2 mm thick), then dried at 80 °C for 12 h. Each electrode contained 4 mg of the electroactive material and had a geometric surface area of 1  $\text{cm}^2$ .

The electrochemical measurements were carried out using a conventional three-electrode system with an aqueous solution (electrolyte: 2 M KOH,  $\text{Na}_2\text{S}_2\text{O}_8/\text{KOH}$ ). A platinum sheet electrode

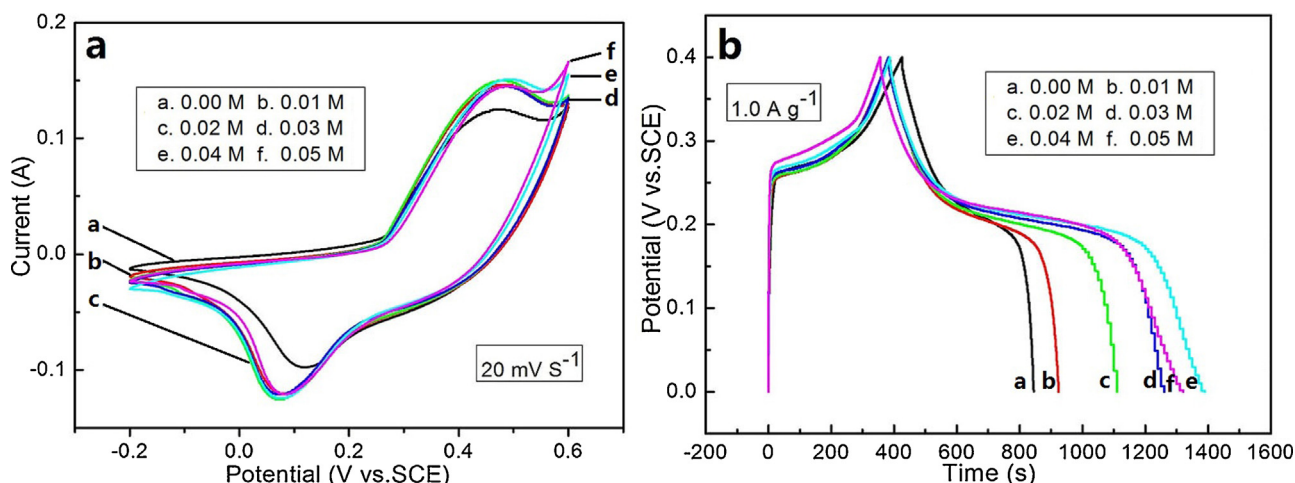


Fig. 1. Cyclic voltammograms (a) and Galvanostatic charge-discharge curves (b) of NiO in 2 M KOH containing different concentration of  $\text{Na}_2\text{S}_2\text{O}_8$ .

(1.5 cm × 1.5 cm) with a surface area of 2.25 cm<sup>2</sup> was used as the counter electrode and a saturated calomel electrode (SCE) served as the reference electrode. The cyclic voltammetry (CV), charge-discharge tests, and electrochemical impedance spectroscopy (EIS) measurements were performed using an electrochemical workstation (CHI660D, Shanghai, China). The cycling performance was tested using a CT2001A battery program controlling test system (China-Land Com. Ltd). The specific capacitance of the electrodes was calculated from the following equation:

$$C_m = \frac{C}{m} = \frac{I \times \Delta t}{\Delta V \times m} \quad (1)$$

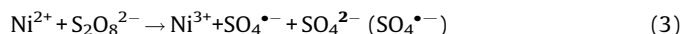
Where  $C_m$  (Fg<sup>-1</sup>) is the specific capacitance,  $C$  is the total capacitance,  $I$ (A) is the discharge current,  $\Delta t$  (s) is the discharge time,  $\Delta V$ (V) represents the potential drop during discharge, and  $m$  (g) is the mass of the active material.

### 3. Results and discussion

Experiment shows that Na<sub>2</sub>S<sub>2</sub>O<sub>8</sub> has the potential as the redox-mediated for the alkaline electrolyte, and suitable for most metal oxides electrodes, this article will mainly exploring the electrochemical performance of NiO electrodes in Na<sub>2</sub>S<sub>2</sub>O<sub>8</sub>/KOH redox-active electrolytes. Detailed electrochemical characterization was realized in order to evaluate electrochemical activity of aforementioned redox active species by various methods. Fig. 1 a displays the CV curves of NiO electrode in a series of Na<sub>2</sub>S<sub>2</sub>O<sub>8</sub>/KOH redox-active electrolytes at the potential scan rate of 20 mVs<sup>-1</sup>. A group of anodic and cathodic peaks were observed from the CV curves no matter the Na<sub>2</sub>S<sub>2</sub>O<sub>8</sub>'s concentration is as low as 0.01 M or as high as 0.05 M in KOH electrolytes, at the same time the area and peak current of CV curves increased with the increasing of the concentration of Na<sub>2</sub>S<sub>2</sub>O<sub>8</sub>. Anodic and cathodic peak currents are correspond to the redox reaction of electrode, the more area and higher peak current of CV curves, the more electrons take part in the redox reaction. At the same time, it is observed that there is no other redox peaks appear when adding redox species, meaning there is no other redox reaction take place on the electrode surface after adding the redox species. As noted above, the number of electrons is increased, but no additional redox reaction; it needs other means to explain this particular phenomenon. The CV curves of NiO electrode in 2 M KOH solutions are showed in Fig. S2a.

In order to explain the increase of electrons but not appear another redox reaction on the CV curves after adding Na<sub>2</sub>S<sub>2</sub>O<sub>8</sub> into KOH electrolyte, the galvanostatic charge-discharge measurements were performed. Fig. 1 b displays the charge-discharge curves of NiO electrode in a series of Na<sub>2</sub>S<sub>2</sub>O<sub>8</sub>/KOH redox-active electrolytes at different current densities. As the Na<sub>2</sub>S<sub>2</sub>O<sub>8</sub> concentration increased from 0.00 to 0.04 M, the discharge time are gradually increased, but it reduced when further increasing the Na<sub>2</sub>S<sub>2</sub>O<sub>8</sub> concentration to 0.05 M. The specific capacitance, evaluated at a high current density of 1 Ag<sup>-1</sup> from charge-discharge curves, are 835, 1346.5, 1820, 2202.5, 2507.5, and 2407.5 Fg<sup>-1</sup>, respectively, corresponding to the coulombic efficiency of 100%, 161%, 218%, 264%, 300%, and 288%, respectively. The specific capacitance showed a decreasing trend after a period of increased, the reason is when the Na<sub>2</sub>S<sub>2</sub>O<sub>8</sub> concentration is lower, the contribution of the redox reaction from Na<sub>2</sub>S<sub>2</sub>O<sub>8</sub> is relatively lower, then resulted a low specific capacitance. However, high charge-discharge current density will cause high concentration polarization, leading to a low rate property and poor electrochemical stability. In addition to the prolonged of discharging time, the charging time is slightly reduced; to explain this phenomenon, the reaction process is a key. When electrolyte is pure KOH aqueous solution, the charge-discharge process can be expressed as the

equation (2), corresponding to the reversible redox reaction of Ni<sup>2+</sup>/Ni<sup>3+</sup>, at this time the charge-discharge time is roughly equal. When the Na<sub>2</sub>S<sub>2</sub>O<sub>8</sub> is added into the KOH electrolyte, the S<sub>2</sub>O<sub>8</sub><sup>2-</sup> will take part in the above reaction. During charging process, the Ni<sup>2+</sup> is oxidized into Ni<sup>3+</sup>, meanwhile, the Ni<sup>2+</sup> can be the initiator reacted with the S<sub>2</sub>O<sub>8</sub><sup>2-</sup>, the reactions are given by the equation (3). Due to the two steps reaction, the charging time is shorted. During discharging process, the Ni<sup>3+</sup> is reduced into Ni<sup>2+</sup>, and then it will be oxidized into Ni<sup>3+</sup> by S<sub>2</sub>O<sub>8</sub><sup>2-</sup>, the Ni<sup>3+</sup> will repeat the backward reaction of process (2), thus the discharging time is extended. The whole schematic is illustrated in the Fig. 2. The galvanostatic charge-discharge curves shows that the effect of adding Na<sub>2</sub>S<sub>2</sub>O<sub>8</sub> will fade at higher concentration (0.05 M), which probably due to the occurred of concentration polarization phenomenon. Increase diffusion rate is a way to verify the occurred of concentration polarization phenomenon, and avoid it. Therefore, we need to explore the effect of diffusion rate. As a comparison, the charge-discharge curves of NiO electrode in 2 M KOH solutions are showed in the Fig. S2b.



Both increasing temperature and forced convection can improve the diffusion rate, in this experiment the diffusion rate was increased by raising the temperature. Fig. 3 shows the electrochemical properties of the NiO electrode at different temperatures (20 °C, 40 °C, and 60 °C) in 2 M KOH containing 0.03 M Na<sub>2</sub>S<sub>2</sub>O<sub>8</sub>. It is noted that sodium persulfate may decompose and generate sodium sulfate when the temperatures is above 60 °C. Fig. 3 a is the CV curves of NiO electrode at different temperatures, the area of CV curves increased with the raising of temperature. This phenomenon shows that there is more active substance participated in the reaction at high temperatures, and more electrons are released, which were also reflected in the Fig. 3 b. In the galvanostatic charge-discharge curves at 10 Ag<sup>-1</sup>, both the charging time and discharging time has been extended at high temperatures. The charging time are 20 s, 25.6 s, and 32.1 s at different temperature, corresponding to the discharging time of 22.9 s, 30 s, and 32.1 s, respectively. The specific capacitance, evaluated at a high current density of 10 Ag<sup>-1</sup> from charge-discharge curves, are 550, 750, and 802 Fg<sup>-1</sup>, corresponding to the coulombic efficiency of 100%, 136%, and 146%, respectively. Fig. 3 c is the EIS plots of NiO at different temperature; and the inset shows the semicircle evident at high frequency. All the impedance spectra are similar, composed of one semicircle at high frequency followed by a linear component at low frequency. The semicircular in high frequency region represents the charge transfer resistance; the

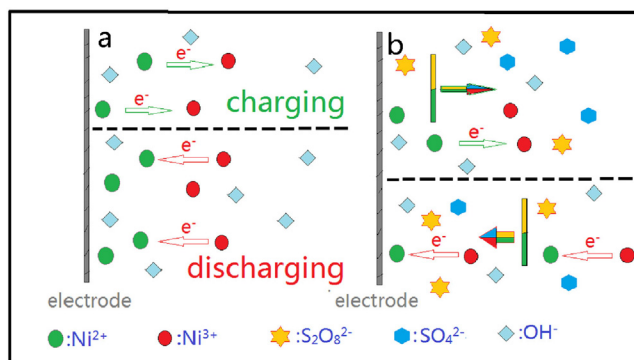
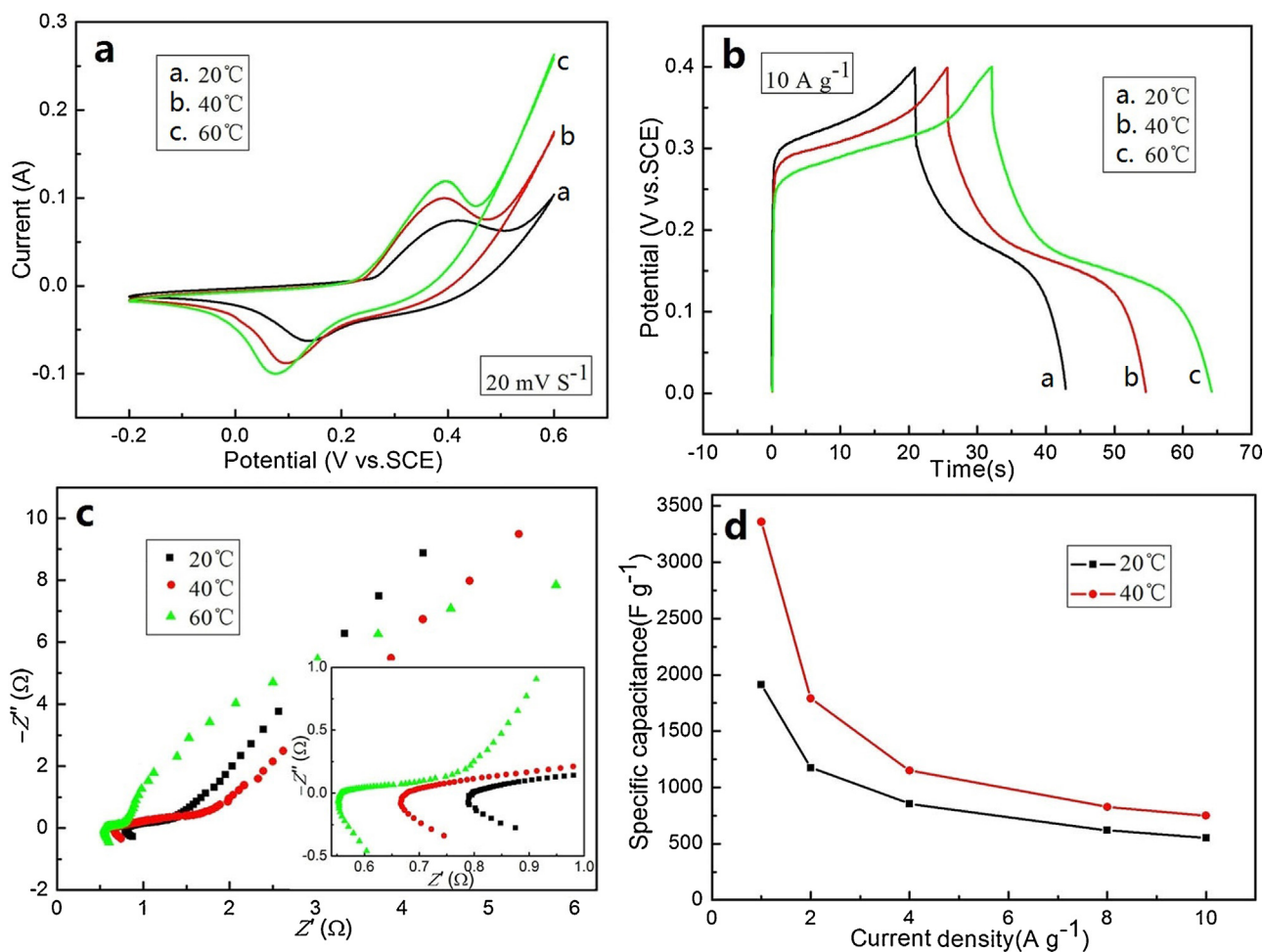


Fig. 2. Schematic illustration of the charge-discharge of NiO in 2 M KOH (part a) and 2 M KOH containing Na<sub>2</sub>S<sub>2</sub>O<sub>8</sub> mixed solution (part b).



**Fig. 3.** CV curves at  $20 \text{ mV s}^{-1}$  (a), galvanostatic charge-discharge curves at  $10 \text{ A g}^{-1}$  (b), EIS plots (c), and the specific capacitance calculated from discharge curves at different current densities (d) of NiO electrode at different temperature in  $2 \text{ M KOH}$  containing  $0.03 \text{ M Na}_2\text{S}_2\text{O}_8$  mixed solution.

straight line of low frequency represents mass transfer impedance. The intrinsic impedance of the electrode can be calculated from the intersection of impedance spectrum and the real axis, which includes ion impedance of electrolyte, intrinsic impedance of the electrode materials and the contact resistance of active substances and collector. It can be clearly observed that with the raised

temperature, the intrinsic impedance of the electrode is decreased. This is due to the ions and charge have a greater movement rate at high temperature, and it also accelerate of ions embed and prolapsed at the electrode surface. The specific capacitance calculated from discharge curves at different current densities of NiO electrode are shown in Fig. 3d, it is obvious that the

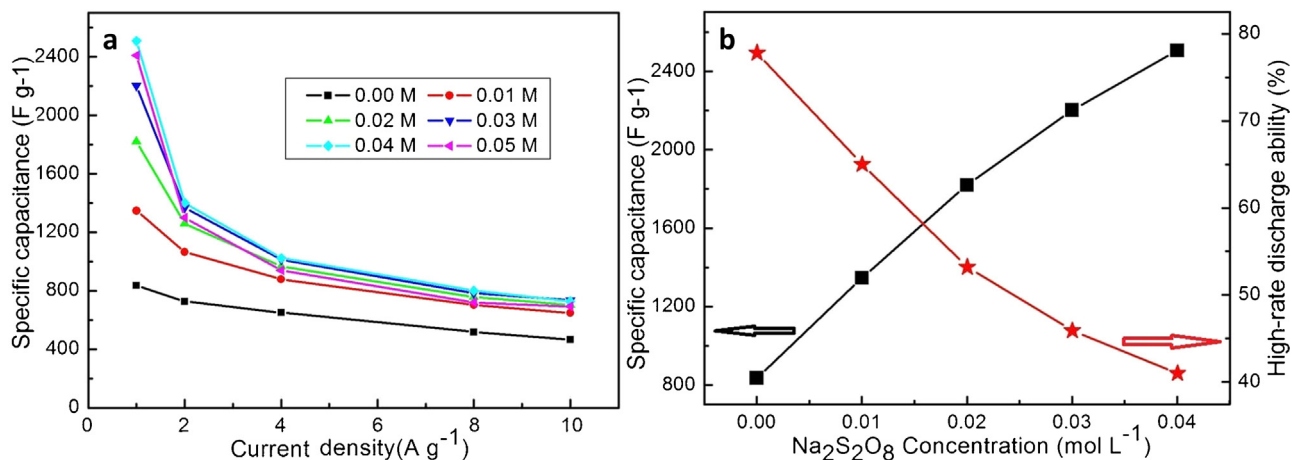


**Fig. 4.** the specific capacitance calculated from discharge curves at different current densities (a) specific capacitance and high-rate discharge ability (b) for the system of NiO electrode in  $2 \text{ M KOH}$  containing different concentrations of  $\text{Na}_2\text{S}_2\text{O}_8$  mixed solution.



temperature of electrolyte has a significant influence on the specific capacitances. At the same current density, specific capacitance increased with the temperature. Since the  $\text{Na}_2\text{S}_2\text{O}_8$  will decompose above  $60^\circ\text{C}$ , this part test data is inaccurate; the figure not shows the specific capacitance at this temperature. These experiments demonstrate that raised temperatures can improve the diffusion rate and moderate the concentration polarization phenomenon; it results in a better electrochemical performance. In addition to change the temperature, forced convection is another means to improve the diffusion rate, and those experiment data are show in Fig.S3. All those experimental data illustrate raising temperatures and force convection can improve the diffusion rate, it is also demonstrate that diffusion is the control factor of charge-discharge process, thus advance the diffusion rate could avoid concentration polarization phenomenon and achieve a good rate capability.

Fig. 4a is the variation of specific capacitance as a function of current densities for NiO electrode in 2 M KOH containing different concentrations of  $\text{Na}_2\text{S}_2\text{O}_8$  mixed solution, the specific capacitance is calculated from the discharge curves. The figure shows that with the increase of the concentration, the specific capacitance is increased; however, the capacitance retention rate is disaccord, at lower current densities the capacitance is obvious upgrade. This is because when the  $\text{Na}_2\text{S}_2\text{O}_8$  concentration is lower; the contribution from  $\text{Na}_2\text{S}_2\text{O}_8$  is lower, resulting in a low specific capacitance. However, high concentration and charge-discharge current density will cause high concentration polarization, leading to a low rate property and poor electrochemical stability. Next, the greater the current density, the faster the oxidation-reduction reaction rate at the electrode surface, at this point, the migration rate of electrolyte ions became the rate-controlling factor. When the ion migration rate even less than the reaction rate of electrode surface, the reaction is insufficient, which caused the lower capacitance. High concentration of  $\text{Na}_2\text{S}_2\text{O}_8$  has obvious effect to the system, but there is an overlap trend of the curves at higher current density, which suggests the effect of  $\text{Na}_2\text{S}_2\text{O}_8$  has fade at higher concentration. Take the economic into consideration, choice fewer active substances to achieve the best results is the right way. In addition, if the high-rate discharge ability (HRD) of the electrode is defined as the ratio of discharge specific capacitance at  $4\text{ A g}^{-1}$  to that at  $1\text{ A g}^{-1}$ , the HRD for the system containing different concentrations of  $\text{Na}_2\text{S}_2\text{O}_8$  mixed solution, are 78%, 65%, 53%, 46%, and 41%, respectively. The typical data about the specific capacitance and HRD for the system containing different concentrations of  $\text{Na}_2\text{S}_2\text{O}_8$  mixed solution are shown in Fig. 4b, the left

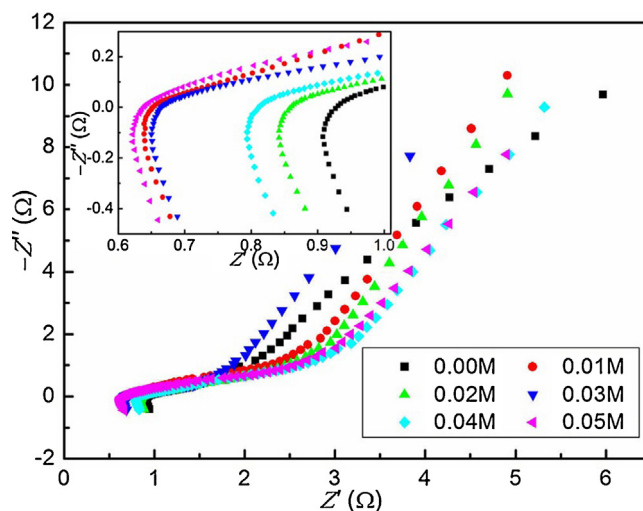


Fig. 5. Nyquist plot for the system of NiO electrode in 2 M KOH containing different concentrations of  $\text{Na}_2\text{S}_2\text{O}_8$  mixed solution.

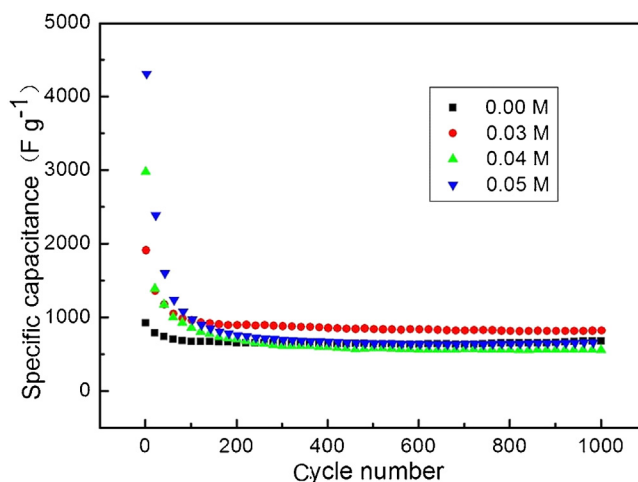


Fig. 6. cycling performance of NiO electrode in 2 M KOH containing different concentrations of  $\text{Na}_2\text{S}_2\text{O}_8$  mixed solution.

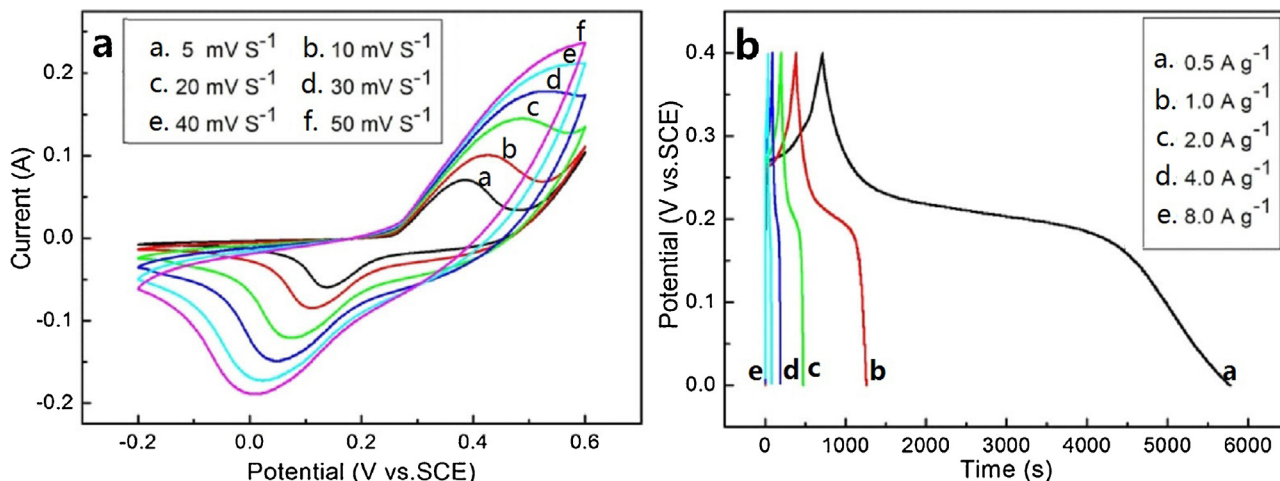


Fig. 7. CV curves (a) and galvanostatic charge-discharge curves (b) of NiO electrode in 2 M KOH containing 0.03 M  $\text{Na}_2\text{S}_2\text{O}_8$  mixed solution.

data is the specific capacitance at  $1 \text{ A g}^{-1}$  of NiO electrode in 2 M KOH containing different concentrations of  $\text{Na}_2\text{S}_2\text{O}_8$ , the specific capacitance increased trend was almost linearly, and reached  $2500 \text{ F g}^{-1}$  at 0.04 M, there is 3-fold increase than without added  $\text{Na}_2\text{S}_2\text{O}_8$ . In summary, the  $\text{Na}_2\text{S}_2\text{O}_8$  concentration has a significant influence on the specific capacitance, coulombic efficiency and rate property. High  $\text{Na}_2\text{S}_2\text{O}_8$  concentration facilitates a high specific capacitance and coulombic efficiency, but worsens rate property and electrochemical stability. Therefore, only the  $\text{Na}_2\text{S}_2\text{O}_8$

**Table 1**

Charge and discharge time for NiO electrode in 2 M KOH containing 0.03 M  $\text{Na}_2\text{S}_2\text{O}_8$  mixed solution, calculated from galvanostatic charge-discharge curves at different current density.

Current density ( $\text{A g}^{-1}$ )	Charge time (s)	Discharge time (s)
$0.5 \text{ A g}^{-1}$	715	5054
$1 \text{ A g}^{-1}$	394	877
$2 \text{ A g}^{-1}$	200	273.6
$4 \text{ A g}^{-1}$	91	101.21
$8 \text{ A g}^{-1}$	33.5	39.13

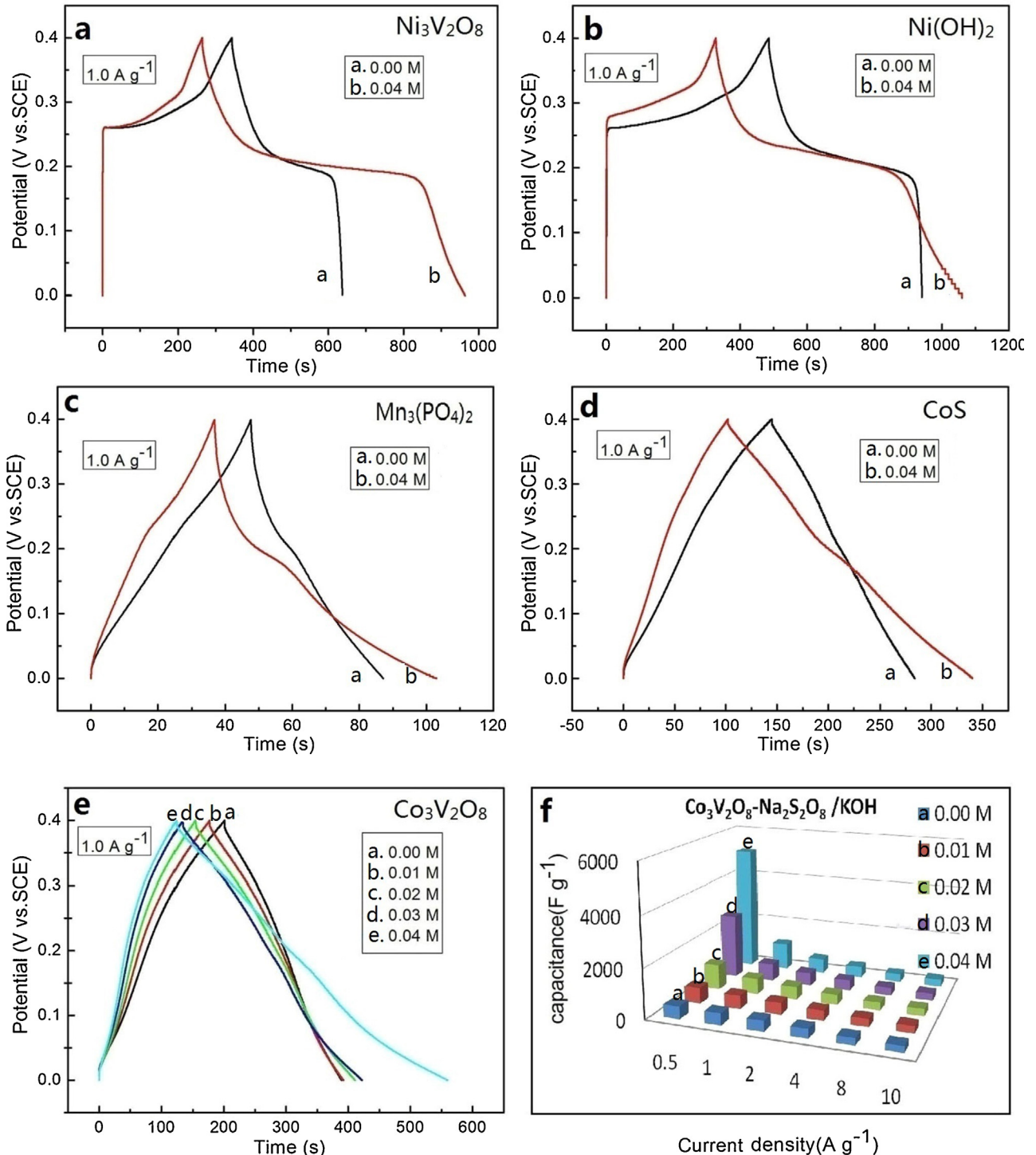


**Fig. 8.** Galvanostatic charge-discharge curves of different electrodes (a, b, c, d, and e) and the specific capacitance of  $\text{Co}_3\text{V}_2\text{O}_8$  electrode at different current densities in 2 M KOH containing different concentrations of  $\text{Na}_2\text{S}_2\text{O}_8$  mixed solution (f).

concentration is proper, the capacitance, coulombic efficiency and rate property can be compromised.

Fig. 5 shows the Nyquist plots of NiO electrode using 2 M KOH and 2 M KOH containing different concentrations of  $\text{Na}_2\text{S}_2\text{O}_8$  mixed solution as the electrolyte. The inset shows the semicircle evident at high frequency. The intrinsic impedance of the electrode can be obtained from the intersection of impedance spectrum and the real axis, the figure shows that the intrinsic impedance of the NiO electrode is the largest in pure KOH electrolyte. With the increasing of the  $\text{Na}_2\text{S}_2\text{O}_8$  concentrations, the intrinsic impedance shows a decreasing trend, this is due to the large active ion concentration of the electrolyte can shorten the diffusion distance of ions and charge. The diffusive resistance (Warburg impedance) of the NiO electrode that used active electrolyte, represented by the straight line at low frequency (the greater of the slope of the linear portion, the smaller of the diffusive impedance), was lower than that in pure KOH electrolyte, this is because the large concentrations of ions and charge in electrolyte can make the transfer of ions more convenient. Accordingly, a facile faradaic redox reaction would be taken, and a good electrochemical property could be realized for the NiO electrode by adding  $\text{Na}_2\text{S}_2\text{O}_8$  into KOH electrolyte.

The electrochemical stability is a very important factor for determining the capacitive properties of pseudocapacitors with the introduction of additive into electrolyte. The cycling stability of the NiO electrode was further investigated by galvanostatic charge-discharge between 0 and 0.4 V at a current density of  $1.0 \text{ A g}^{-1}$ . As shown in Fig. 6, when the active substances is added into 2 M KOH electrolyte, the capacitance is raised, which indicates that the addition of  $\text{Na}_2\text{S}_2\text{O}_8$  have an effect to the electrode material, but the growth of specific capacitance will be reduced after the initial 200 cycles, and the loss of capacitance is higher than not add active substances, fortunately, after 1000 cycles the specific capacitance almost remains a high value.

Fig. 7a shows the CV curves of NiO electrode in a mixed solution containing 2 M KOH and 0.03 M  $\text{Na}_2\text{S}_2\text{O}_8$ . A pair of redox peaks is visible in each voltammogram, suggesting that the measured capacitance is mainly based on the redox mechanism. The peak current increased with the increase of the scan rate, which suggests that the kinetics of the interfacial Faradic redox reactions and the rates of electronic and ionic transport are rapid enough in the present scan rates. The shape of the CV curves is not significantly influenced by the increase of the scan rates, which indicates the improved mass transportation and electron conduction of the host materials. Fig. 7b shows the galvanostatic charge-discharge curves at different current densities. The corresponding specific capacitances of the NiO electrode, calculated from the discharge time according to eqn (1), are 6317.5, 2202.5, 1368, 1012, and  $783 \text{ F g}^{-1}$  at the discharge current densities of 0.5, 1, 2, 4, and  $8 \text{ A g}^{-1}$ , respectively. The specific capacitance gradually decreased at higher current density due to the incremental (IR) voltage drop, and insufficient active material being involved in the redox reaction at higher current density, result in the reaction is not very complete. The charge and discharge time for NiO electrode in the mixed solution of 2 M KOH and 0.03 M  $\text{Na}_2\text{S}_2\text{O}_8$  are shown in Table 1, like others electrode materials, the charge and discharge time are reduced with the increases of current density, but there is one thing should be pay attention, the charge and discharge time is asymmetrical, the discharge time is much less than the charge time, especially in smaller current density. The system can be charged quickly, and discharged slowly, which means that the promise can be offered to realize a battery-type supercapacitor.

It is worth noting that  $\text{Na}_2\text{S}_2\text{O}_8/\text{KOH}$  redox-active electrolytes not only suitable for the NiO electrode, but also for most metal oxides electrode. Fig. 8(a-e) shows the galvanostatic charge-discharge curve of the  $\text{Ni}_3\text{V}_2\text{O}_8$ ,  $\text{Ni}(\text{OH})_2$ ,  $\text{Mn}_3(\text{PO}_4)_2$ , CoS, and  $\text{Co}_3\text{V}_2\text{O}_8$  electrode in a mixed solution containing 2 M KOH and

different concentrations of  $\text{Na}_2\text{S}_2\text{O}_8$ , respectively, the figure shows the redox-mediated electrolyte are suitable for each electrode materials, and emerged the phenomenon of charging time shortened and the discharge time extended, all those electrodes have the same mechanism with the NiO electrode in redox-active electrolytes. Fig. 8f shows the specific capacitance of  $\text{Co}_3\text{V}_2\text{O}_8$  electrode at different current densities in 2 M KOH containing different concentrations of  $\text{Na}_2\text{S}_2\text{O}_8$  mixed solution, the three-dimensional figure clearly shows the trend of specific capacitance, at lower current densities and relatively large concentration of the  $\text{Na}_2\text{S}_2\text{O}_8$ , the effect of redox-active electrolytes is obvious, this is also consistent with the results of the NiO electrode. The CV curves and the EIS plots of  $\text{Co}_3\text{V}_2\text{O}_8$  electrode in 2 M KOH containing different concentration of  $\text{Na}_2\text{S}_2\text{O}_8$  are show in Fig. S4.

#### 4. Conclusion

In summary, a simple and effective method to enhance the electrochemical performance of metal oxide electrode through introducing  $\text{Na}_2\text{S}_2\text{O}_8$  into the conventional KOH electrolyte has been successfully introduced. As both solid electrode and liquid electrolyte can contribute to the pseudocapacitance simultaneously, an ultrahigh capacitive performance has been realized. The NiO- $\text{Na}_2\text{S}_2\text{O}_8/\text{KOH}$  system exhibit an ultrahigh specific capacitance, the specific capacitance is 3-fold increase than without added  $\text{Na}_2\text{S}_2\text{O}_8$ , reached  $6317.5 \text{ F g}^{-1}$  at  $0.5 \text{ A g}^{-1}$  in mixed solution containing 2 M KOH and 0.03 M  $\text{Na}_2\text{S}_2\text{O}_8$ . More valuable is the redox-active electrolytes system is suitable for most metal oxides electrodes (metal sulfide, vanadate, and phosphate electrode et al), and make the charged quickly, and discharged slowly, which means the redox-active electrolytes system can applied in the battery-type supercapacitor.

#### Acknowledgments

This work was supported by the National Natural Science Foundation of China (no. 51362018,21163010).

#### Appendix A. Supplementary data

Supplementary data associated with this article can be found, in the online version, at <http://dx.doi.org/10.1016/j.electacta.2015.10.161>.

#### References

- [1] J.R. Miller, R.A. Outlaw, B.C. Holloway, *Science* 329 (2010) 1637.
- [2] D. Pech, M. Brunet, H. Durou, P. Huang, V. Mochalin, Y. Gogotsi, *Nat. Nanotechnol.* 5 (2010) 651.
- [3] T. Brezesinski, J. Wang, S.H. Tolbert, B. Dunn, *Nat. Mater.* 9 (2010) 146.
- [4] L.Q. mai, F. Yang, Y.L. Zhao, X. Xu, L. Xu, Y.Z. Luo, *Nat. Comms.* 2 (2011) 381.
- [5] Q.T. Qu, S.B. Yang, X.L. Feng, *Adv. Mater.* 23 (2011) 5574.
- [6] W. Chen, Z.L. Fan, L. Gu, X.H. Bao, C.L. Wang, *Chem. Commun.* 46 (2010) 3905.
- [7] J. Bae, M.K. Song, Y.J. Park, J.M. Kim, M.L. Liu, Z.L. Wang, *Angew. Chem., Int. Ed.* 50 (2011) 1683.
- [8] J.S. Huang, B.G. Sumpter, V. Meunier, *Angew. Chem. Int. Ed.* 47 (2008) 520.
- [9] S.J. Ding, T. Zhu, J.S. Chen, Z.Y. Wang, C.L. Yuan, X.W. Lou, *J. Mater. Chem.* 21 (2011) 6602.
- [10] H.L. Wang, H.S. Casalongue, Y.Y. Liang, H.J. Dai, *J. Am. Chem. Soc.* 132 (2010) 7472.
- [11] L.B. Kong, M.C. Liu, J.W. Lang, M. Liu, Y.C. Luo, L. Kang, *J. Solid State Electrochem.* 15 (2011) 571.
- [12] S.K. Chang, K.T. Lee, Z. Zainal, K.B. Tan, N.A. Yusof, W.M.D.W. Yusoff, J.F. Lee, N.L. Wu, *Electrochim. Acta* 67 (2012) 67.
- [13] H. Jiang, T. Zhao, C.Z. Li, J. Ma, *J. Mater. Chem.* 21 (2011) 3818.
- [14] M.F. Shao, F.Y. Ning, Y.F. Zhao, J.W. Zhao, M. Wei, D.G. Evans, X. Duan, *Chem. Mater.* 24 (2012) 1192.
- [15] Y.H. Zhu, E.H. Liu, Z.Y. Luo, T.T. Hu, T.T. Liu, Z.P. Li, Q.L. Zhao, *Electrochim. Acta* 118 (2014) 106.
- [16] T.Y. Wei, C.H. Chen, H.C. Chen, S.Y. Lu, C.C. Hu, *Adv. Mater.* 22 (2010) 347.
- [17] C.C. Hu, K.H. Chang, M.C. Lin, Y.T. Wu, *Nano Lett.* 6 (2006) 2690.

- [18] X. Zhang, W. Shi, J. Zhu, D.J. Kharistal, W. Zhao, B.S. Lalia, H.H. Hng, Q. Yan, *ACS Nano* 5 (2011) 2013.
- [19] X. Lu, G. Wang, T. Zhai, M. Yu, J. Gan, Y. Tong, Y. Li, *Nano Lett.* 12 (2012) 1690.
- [20] M. Vezvaie, P. Kalisvaart, H. Fritzsche, Z. Tun, D. Mitlin, *J ELECTROCHEM SOC* 161 (2014) A798.
- [21] Q. Qu, P. Zhang, B. Wang, Y. Chen, S. Tian, Y. Wu, R. Holze, *J. Phys Chem C* 113 (2009) 14020.
- [22] R.K. Selvan, I. Perelshtein, N. Perkas, A. Gedanken, *J. Phys Chem C* 112 (2008) 1825.
- [23] K.K. Purushothaman, M. Cuba, G. Muralidharan, *J. Materresbull* 11 (2012) 3348.
- [24] Q.F. Wang, B. Liu, X.F. Wang, S.H. Ran, L.M. Wang, D. Chen, G.Z. Shen, *J. Mater. Chem* 22 (2012) 21647.
- [25] Q.H. Wang, L.F. Jiao, H.M. Du, Y.C. Si, Y.J. Wang, H.T. Yuan, *J. Mater. Chem.* 22 (2012) 21387.
- [26] S.D. Perera, B. Patel, J. Bonso, M. Grunewald, J.P. Ferraris, K.J. Balkus, *ACS Appl Mater Interfaces* 3 (2011) 4512.
- [27] D. Choi, G.E. Blomgren, P.N. Kumta, *Adv. Mater.* 18 (2006) 1178.
- [28] J. Yan, Z. Fan, W. Sun, G. Ning, T. Wei, Q. Zhang, R. Zhang, L. Zhi, F. Wei, *Adv. Funct. Mater.* 22 (2012) 2632.
- [29] M.C. Liu, L.B. Kong, X.J. Ma, X.M. Li, C. Lu, Y.C. Luo, L. Kang, *New. J. Chem.* 36 (2012) 1713.
- [30] L. Wang, Z.H. Dong, Z.G. Wang, F.X. Zhang, J. Jin, *Adv. Funct. Mater.* 23 (2013) 2758.
- [31] H.J. Tang, J.G. Wang, H.J. Yin, H.J. Zhao, D. Wang, Z.Y. Tang, *Adv. Mater.* 27 (2015) 1117.
- [32] J.W. Lang, L.B. Kong, W.J. Wu, Y.C. Luo, L. Kang, *Chem. Commun.* 35 (2008) 4213.
- [33] S. Roldán, C. Blanco, M. Granda, R. Menéndez, R. Santamaría, *Angew. Chem. Int. Ed.* 50 (2011) 1699.
- [34] J.H. Wu, et al., *J. Mater. Chem.* 22 (2012) 19025.
- [35] S.T. Senthilkumar, R.K. Selvan, N. Ponpandian, J.S. Melo, *RSC Adv.* 2 (2012) 8937.
- [36] S.T. Senthilkumar, et al., *Mater. Chem. A* 1 (2013) 1086.
- [37] L.H. Su, X.G. Zhang, B.G.A.O. Mi, *Chem. Chem. Phys.* 11 (2009) 2195.
- [38] C.M. Zhao, W.T. Zheng, X. Wang, H.B. Zhang, X.Q. Cui, H.T. Wang, *Sci. Rep.* 3 (2013) 2986.
- [39] Y.Q. Gao, N.Y. Gao, Y. Deng, D.Q. Yin, Y.S. Zhang, *Environmental Science and Pollution Research* 11 (2015) 8693.
- [40] Y.Q. Gao, N.Y. Gao, Y. Deng, Y.Q. Yang, Y. Ma, *Chem Eng J* 195 (2012) 248.
- [41] X.G. Gu, S.G. Lu, Q. Sui, Z.W. Miao, K.F. Lin, Y.D. Liu, Q.S. Luo, *Ind Eng Chem Res.* 51 (2012) 7196.
- [42] X.X. Jiang, Y.L. Wu, P. Wang, H.J. Li, W.B. Dong, *Environ Sci Pollut Res.* 20 (2013) 4947.
- [43] A. Tsitonaki, B. Petri, M. Crimi, et al., *Crit. Rev. Env. Sci. Tec.* 40 (2010) 55.